Electronic Supplementary Information

A mononuclear nonheme cobalt(III)-hydroperoxo complex with an amphoteric reactivity in electrophilic and nucleophilic oxidative reactions

Woon-Young Tcho,[a,§] Bin Wang,[a,§] Yong-Min Lee,[a] Kyung-Bin Cho,[a]
Jason Shearer*[,b] and Wonwoo Nam*[,a]

[a]*Department of Chemistry and Nano Science, Center for Biomimetic Systems, Ewha Womans University, Seoul 03760, Korea*
[b]*Department of Chemistry, University of Nevada, Reno, NV 89557, United States*

*E-mail: wwnam@ewha.ac.kr (W.N.) and shearer@unr.edu (J.S.)

[§] These authors contributed equally to this study.

Table of Contents

Experimental Section

Materials. Commercially available chemicals were used without further purification unless otherwise indicated. Solvents were dried according to published procedures and distilled under Ar prior to use.[S1] H_2O_2 (30 wt. % in water) was purchased from Sigma-Aldrich. The 12-TMC ligand and the corresponding cobalt(II) complex, $[Co^{II}(12\text{-TMC})](CF_3SO_3)_2$, were prepared according to the reported methods.[S2]

Instrumentation. UV-Vis spectra were recorded on a Hewlett Packard Agilent 8453 UV-visible spectrophotometer equipped with a circulating water bath or an UNISOKU cryostat system (USP-203; UNISOKU, Japan). Electrospray ionization mass spectra (ESI-MS) were collected on a Thermo Finnigan (San Jose, CA, USA) LCQ Advantage MAX quadrupole ion trap instrument, by infusing samples directly into the source at 20 μL/min using a syringe pump. The spray voltage was set at 4.7 kV and the capillary temperature at 80 °C. X-band CW-EPR spectra were recorded at 5 K using an X-band Bruker EMX-plus spectrometer equipped with a dual mode cavity (ER 4116DM). Low temperatures were achieved and controlled with an Oxford Instruments ESR900 liquid He quartz cryostat with an Oxford Instruments ITC503 temperature and gas flow controller. The experimental parameters for EPR spectra were as follows: Microwave frequency = 9.646 GHz, microwave power = 1.0 mW, modulation amplitude = 10 G, gain = 1×10^4, modulation frequency = 100 kHz, time constant = 40.96 ms and conversion time = 85.00 ms. ^1H NMR spectra were measured with a Bruker model digital AVANCE III 400 FT-NMR spectrometer. Product analysis was performed with an Agilent Technologies 6890N gas chromatograph (GC) (HP-5 column, 30 m × 0.32 mm × 0.25 μm film thickness) with a flame ionization detector and Thermo Finnigan (Austin, Texas, USA) FOCUS DSQ (dual stage quadrupole) mass spectrometer interfaced with Finnigan FOCUS gas chromatograph (GC-MS). High performance liquid chromatography (HPLC) analysis was performed on Waters DIOMEX Pump Series P580 equipped with a variable wavelength UV-200 detector and SunFire C18 5 μm column (4.6 mm × 25 mm).

X-Ray Absorption Spectroscopy. Cobalt K-edge XAS studies were performed on the solutions of $[(12\text{-TMC})Co^{III}(OOH)]^{2+}$ (**2**, 2.0 mM). Solutions were injected into aluminum sample holders at low temperature with Kapton tape windows, and quickly frozen in liquid nitrogen. Data were collected on beamline 2-2 at the Stanford Synchrotron Radiation Laboratory. Light was monochromized using a Si(111) double monochromator, which was detuned 40% to eliminate higher order harmonics. Samples were maintained at 20 K throughout data collection with the use of a He Displex closed cycle cryostat. All data were measured in fluorescence mode using a 13-element solid state Ge detector (Canberra). Total count rates were maintained under 30 kHz, and therefore deadtime corrections had no effect on the data. For EXAFS spectra, data were collected in 10 eV steps in the pre-edge region (7510 – 7700 eV), 0.3 eV steps in the edge region (7700 – 7720 eV), 1 eV in the near edge region (7720 – 7740), and 0.05 k steps in the far edge region (7740 – 16.5 *k*). XANES spectra were obtained in 10 eV steps in the pre-edge region (7510 – 7700 eV), 0.3 eV steps in the edge region (7700 – 7730 eV), and 0.5 eV in the near edge region (7730 – 7810). The data set reported represents the sum of 15 individual data sets. Prior to data averaging, each individual detector channel from each data set was inspected for data consistency. No perceptible photodecomposition was noted for the sample.

Data were analyzed using the XAS analysis package *EXAFS123* as previously described.[S3] All data were calibrated against the simultaneously acquired spectrum of Co-foil (first inflection point set to 7709 eV). XANES spectra for all compounds reported below were analyzed by interpolating the experimental data in 0.05 eV step-sizes. We estimate an error in the reported edge positions of ~0.1 eV in these measurements. No data extrapolation was performed for the EXAFS analysis. All known monochromator glitches were removed prior to data analysis. Although collected to 16.5 *k*, EXAFS data were only analyzed to 14.3 *k*. Reported fits to the data in the manuscript are based on unfiltered $k^3(\chi)$ refinements.

Density Functional Theory Calculations

Density functional theory (DFT)[S4] calculations were performed using the B3LYP functional[S5] as implemented in the Gaussian 09 (G09) package.[S6] The geometries were optimized using the Def2-SVP basis set.[S7] The stationary points were confirmed by frequency calculations, and the transition states were connected with the ground states on both sides by performing IRC calculations and continuing relaxing the geometry down to the ground state from the end geometry obtained by IRC. The high molecular charge (2+) made it necessary to perform the optimizations in solvent to avoid potential artificial results, namely DFT self-interaction errors.[S8] Solvent (acetonitrile) effects were included using CPCM model[S9] with UFF cavity, per G09 default. Single-point energy evaluations on the optimized geometry were done with the Def2-TZVPP basis set.[S7] The zero-point vibrational energies (Z_0), the temperature dependent vibrational energies (E(Thermal)) and the entropy (S) was taken from the frequency calculations at Def2-SVP level. Dispersion effects (Disp) were calculated as a single-point correction at the optimized geometry by using the DFT-D3 program[S10] with Becke and Johnson damping.[S11]

Generation of $[(12\text{-TMC})Co^{III}(O_2)]^+$ (1) and $[(12\text{-TMC})Co^{III}(OOH)]^{2+}$ (2)

$[(12\text{-TMC})Co^{III}(O_2)]^+$ (**1**) was prepared according to the literature methods.[S2] **1** was generated by reacting $[Co^{II}(12\text{-TMC})(CF_3SO_3)_2]$ (40 mg; 0.068 mmol) with H_2O_2 (30% in water; 0.34 mmol) in the presence of triethylamine (TEA; 0.14 mmol) in CH_3CN (1.0 mL) at –40 °C. Then, precooled Et_2O (40 mL) was added to the solution of $[(12\text{-TMC})Co^{III}(O_2)](CF_3SO_3)$ to yield a purple precipitate at –40 °C. This purple precipitate was washed with Et_2O for three times and dried under an Ar atmosphere. $[(12\text{-TMC})Co^{III}(OOH)]^{2+}$ (**2**) was then generated by adding triflic acid (HOTf; 10 mM) into a solution of **1** (1.0 mM) under an Ar atmosphere in acetone at 0 °C. UV-vis spectrum of the greenish-blue intermediate **2** exhibits electronic absorption bands at 445 ($\varepsilon \approx 120$ M^{-1} cm^{-1}) and 620 nm ($\varepsilon \approx 240$ M^{-1} cm^{-1}).

Kinetic Measurements and Product Analysis. Kinetic measurements for C−H bond activation, sulfoxidation and aldehyde deformation reactions by **2** were performed on a UV-vis spectrophotometer in acetone at 0 °C. Reactions were run in a 1-cm UV cuvette and followed by monitoring UV-vis spectral changes of reaction solutions, and rate constants were determined under pseudo-first-order conditions (e.g., [substrate]/[Co^{III}-OOH] > 10) by fitting the changes in absorbance at 620 nm due to **2**. First-order fitting of the kinetic data allowed us to determine the pseudo-first-order rate constants. The first-order plots were linear for three or more half-lives with the correlation coefficient of $\rho > 0.999$. In each case, it was confirmed that the rate constants derived from at least five independent measurements agreed within an experimental error of ±10%. The pseudo-first-order rate constants increased proportionally with the increase of concentrations of substrates, from which second-order rate constants were determined.

Products formed in the oxidation reaction of substrates by **2** were analyzed by GC. A solution of substrates (100 mM) was added directly to a solution of **2** (1.0 mM) in acetone at 0 °C. Decane (1.0 mM) was then added to the reaction solutions as an internal standard.

References

S1. W. L. F. Armarego and C. L. L. Chai, *Purification of Laboratory Chemicals*, 6th ed.; Pergamon Press: Oxford, 2009.

S2. J. Cho, R. Sarangi, H. Y. Kang, J. Y. Lee, M. Kubo, T. Ogura, E. I. Solomon and W. Nam, *J. Am. Chem. Soc.*, 2010, **132**, 16977.

S3. (a) R. C. Scarrow, B. S. Strickler, J. J. Ellison, S. C. Shoner, J. A. Kovacs, J. G. Cummings and M. J. Nelson, *J. Am. Chem. Soc.*, 1998, **120**, 9237; (b) B. A. Brennan, G. Alms, M. J. Nelson, L. T. Durney and R. C. Scarrow, *J. Am. Chem. Soc.*, 1996, **118**, 9194; (c) R. S. Scarrow and J. Shearer, *EXAFS123, v. 0.4*; University of Nevada, Reno: Reno, NV, 2015.

S4. W. Kohn and L. J. Sham, *Phys. Rev. A*, 1965, **140**, 1133.

S5. (a) A. D. Becke, *Phys. Rev. A*, 1988, **38**, 3098; (b) A. D. Becke, *J. Chem. Phys.*, 1993, **98**, 1372; (c) A. D. Becke, *J. Chem. Phys.*, 1993, **98**, 5648; (d) C. Lee, W. T. Yang and R. G. Parr, *Phys. Rev. B*, 1988, **37**, 785.

S6. M. J. Frisch, G. W. Trucks, H. B. Schlegel, G. E. Scuseria, M. A. Robb, J. R. Cheeseman, G. Scalmani, V. Barone, B. Mennucci, G. A. Petersson, H. Nakatsuji, M. Caricato, X. Li, H. P. Hratchian, A. F. Izmaylov, J. Bloino, G. Zheng, J. L. Sonnenberg, M. Hada, M. Ehara, K. Toyota, R. Fukuda, J. Hasegawa, M. Ishida, T. Nakajima, Y. Honda, O. Kitao, H. Nakai, T. Vreven, J. A. Montgomery, Jr., J. E. Peralta, F. Ogliaro, M. Bearpark, J. J. Heyd, E. Brothers, K. N. Kudin, V. N. Staroverov, T. Keith, R. Kobayashi, J. Normand, K. Raghavachari, A. Rendell, J. C. Burant, S. S. Iyengar, J. Tomasi, M. Cossi, N. Rega, J. M. Millam, M. Klene, J. E. Knox, J. B. Cross, V. Bakken, C. Adamo, J. Jaramillo, R. Gomperts, R. E. Stratmann, O. Yazyev, A. J. Austin, R. Cammi, C. Pomelli, J. W. Ochterski, R. L. Martin, K. Morokuma, V. G. Zakrzewski, G. A. Voth, P. Salvador, J. J. Dannenberg, S. Dapprich, A. D. Daniels, O. Farkas, J. B. Foresman, J. V. Ortiz, J. Cioslowski, and D. J. Fox, *Gaussian 09, Revisions B.01 and D.01*, Gaussian, Inc., Wallingford CT, 2010.

S7. F. Weigend and R. Ahlrichs, *Phys. Chem. Chem. Phys.*, 2008, **7**, 3297.

S8. (a) A. J. Johansson, M. R. A. Blomberg, and P. E. M. Siegbahn, *J. Chem. Phys.*, 2008, **129**, 154301; (b) A. J. Johansson, M. R. A. Blomberg, and P. E. M. Siegbahn, *J. Phys. Chem. C*, 2007, **111**, 12397.

S9. M. Cossi, N. Rega, G. Scalmani and V. Barone, *J. Comput. Chem.*, 2003, **24**, 669.

S10. S. Grimme, J. Antony, S. Ehrlich, and S. Krieg, *J. Chem. Phys.*, 2010, **132**, 154104.

S11. S. Grimme, S. Ehrlich, and L. Goerigk, *J. Comp. Chem.*, 2011, **32**, 1456.

Table S1. EXAFS least square fitting results for $[(12\text{-TMC})\mathrm{Co}^{\mathrm{III}}(\mathrm{OOH})]^{2+}$ (**2**).

No. of fit	coordination/path	R(Å)[a]	σ^2(Å^2)	ΔE_0 (eV)	ε^2 [b]
1	4 Co-N	2.003(4)	0.0058(5)	0.88	0.92
	1 Co-O	1.861(3)	0.0027(3)		
	5 Fe-C	2.80(1)	0.002(2)		
	4 Fe-C	2.93(1)	0.004(1)		

No. of fit	coordination/path	R(Å)[a]	σ^2(Å^2)	ΔE_0 (eV)	ε^2 [b]
2	2 Co-N	1.990(2)	0.0023(4)	0.88	1.15
	3 Co-N	2.066(1)	0.0027(2)		
	1 Co-O	1.860(2)	0.0024(2)		
	5 Fe-C	2.80(1)	0.002(2)		
	4 Fe-C	2.93(1)	0.004(1)		

No. of fit	coordination/path	R(Å)[a]	σ^2(Å^2)	ΔE_0 (eV)	ε^2 [b]
3	5 Co-N	2.005(6)	0.0083(3)	0.83	0.94
	1 Co-O	1.860(2)	0.0024(15)		
	5 Fe-C	2.80(1)	0.002(2)		
	4 Fe-C	2.93(1)	0.004(1)		

[a] The esds are based on the refinement to the fit. Actual errors in bond lengths should be taken as ±0.02 Å. [b] Errors are given by $\varepsilon^2 = [n_{idp}/(n_{idp} - n_p)] \times \text{average}[(y_{data} - y_{model})/\sigma^2]$ where n_{idp} is the number of independent data points, n_p is the number of refined parameters, σ is the estimated uncertaininty in the data, y_{data} is the experimental k^3 EXAFS spectrum and y_{model} is the simulated k^3 EXAFS spectrum. The S_0^2 factor was set at 1.

Table S2. Relative energies of **2** in different spin states *S* in kcal/mol.

S	ΔDef2-SVP	ΔDef2-TZVPP	**ΔE**[a]	ΔZ_0	ΔE(Thermal)[b,c]	-TΔS[c]	ΔDisp	**ΔG**[d]
0	0.00	+0.00	**0.00**	+0.00	+0.00	+0.00	+0.00	**0.00**
1	4.46	+0.32	**4.78**	-2.73	+1.15	-3.74	+2.15	**1.61**
2	4.47	+2.41	**6.88**	-3.50	+1.58	-5.53	+3.99	**3.42**

[a] Electronic energy ΔE at Def2-TZVPP level calculated as the sum of the two previous columns. [b] Temperature dependent vibrational energy. [c] At 298.15 K. [d] Gibb's free energy ΔG calculated as the sum of the five previous columns.

Table S3. Mulliken spin density distribution of **2** in different spin states.

S	Co	$O_{proximal}$	O_{distal}	4 × N	Rest
0	0.00	0.00	0.00	0.00	0.00
1	2.17	-0.11	-0.11	0.05	0.00
2	2.78	0.60	0.30	0.28	0.03

Table S4. Selected geometries of **2** in different spin states in Å and °.

S	Co–$O_{proximal}$	Co–O_{distal}	$O_{proximal}$–O_{distal}	Co–N (average)	Co–$O_{proximal}$–O_{distal}
0	1.86	2.03	1.43	2.04	75.0
1	1.83	2.71	1.38	2.14	114.5
2	2.02	2.88	1.32	2.20	117.3

Table S5. Product yields obtained in the reactions of **2** with CHD, xanthene, thioanisole, and 2-PPA under an Ar atmosphere in acetone at 0 °C.[a]

entry	substrate	product	yield (%)
1	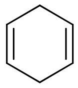	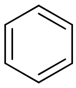	82(5)
2	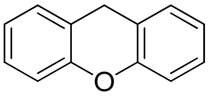	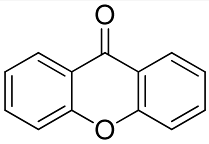	48(4)
3	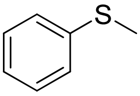	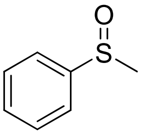	83(5)
4	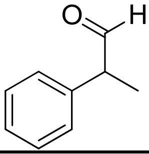	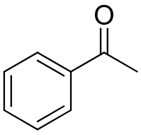	80(6)

[a] Reactions of **2** (1.0 mM) with CHD (100 mM), xanthene (100 mM), thioanisole (200 mM), and 2-PPA (100 mM) were carried out under an Ar atmosphere in acetone at 0 °C. Yields were calculated based on the concentration of **2** used.

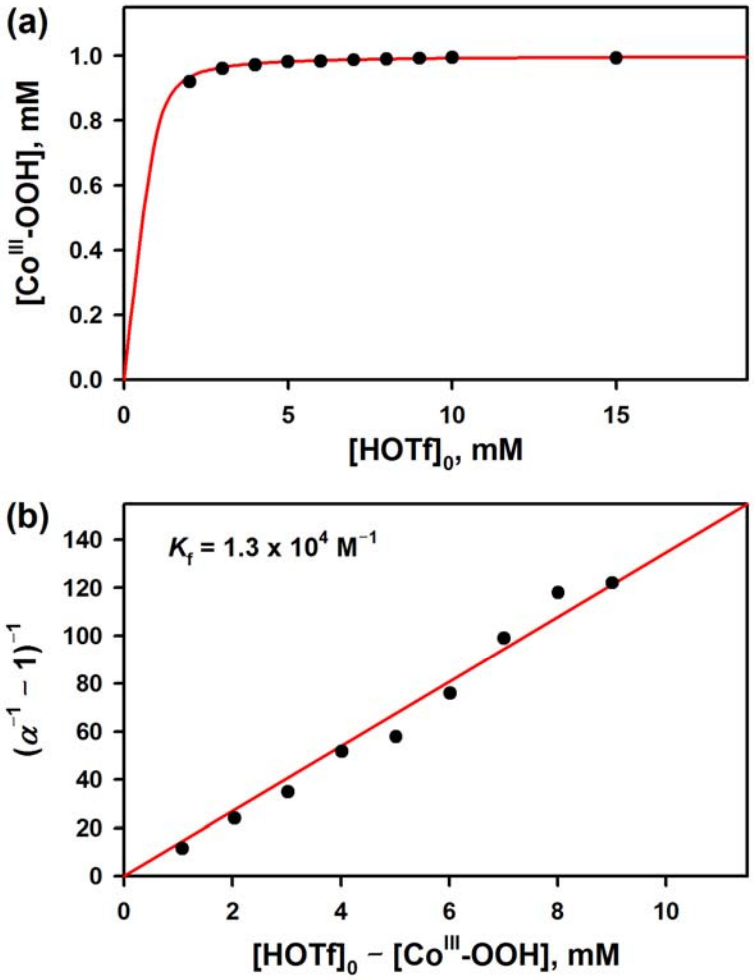

Fig. S1 (a) Plot of concentration of [Co^{III}-OOH]$^{2+}$ (**2**) produced upon addition of HOTf (0 – 15 mM) to a solution of [Co^{III}-O$_2$]$^+$ (1.0 mM) in acetone at –40 °C *vs.* initial concentration of HOTf, [HOTf]$_0$. (b) Plot of (α^{-1} – 1)$^{-1}$ *vs.* [HOTf]$_0$ – [Co^{III}-OOH] (α = [Co^{III}-OOH]/[Co^{III}-O$_2$]$_0$) to determine the formation constant (K_f = [Co^{III}-OOH]/([Co^{III}-O$_2$]×[HOTf])) upon addition of HOTf (0 – 15 mM) into the solution of [Co^{III}-O$_2$]$^+$ (1.0 mM) in acetone at –40 °C.

The formation constant, K_f, is expressed by Eq (S1).

$$K_f = [\mathrm{Co^{III}\text{-}OOH}]/([\mathrm{Co^{III}\text{-}O_2}]\times[\mathrm{HOTf}]) \tag{S1}$$

Eq (S2) is derived from Eq (S1), where [HOTf]$_0$ = [HOTf] + [Co^{III}-OOH], [Co^{III}-O$_2$]$_0$ = [Co^{III}-O$_2$] + [Co^{III}-OOH], and α = [Co^{III}-OOH]/ [Co^{III}-O$_2$]$_0$. [HOTf]$_0$ =and [Co^{III}-O$_2$]$_0$ are the initial concentration of [Co^{III}-O$_2$]$^+$ (**1**) and HOTf, respectively.

$$(\alpha^{-1} - 1)^{-1} = K_f([\mathrm{HOTf}]_0 - [\mathrm{Co^{III}\text{-}OOH}]) \tag{S2}$$

The K_f value is determined from the slope of the linear plot of (α^{-1} – 1)$^{-1}$ against ([HOTf]$_0$ – [Co^{III}-OOH]).

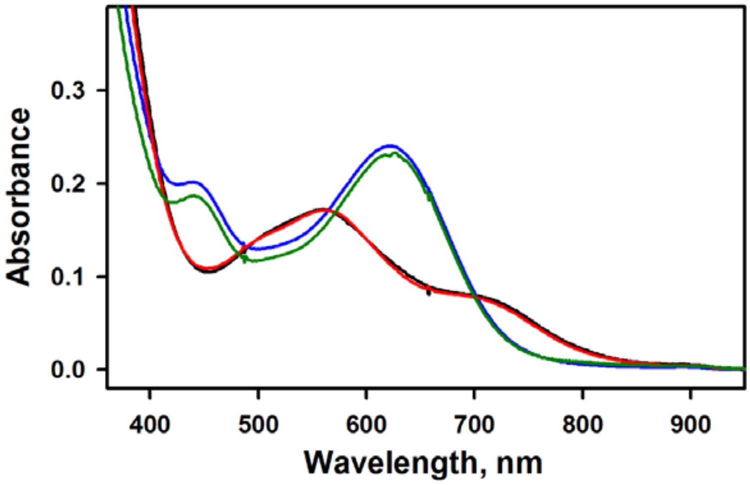

Fig. S2 UV-vis spectral changes showing the interconversion between [(12-TMC)Co^{III}(O$_2$)]$^+$ (**1**) (1.0 mM) and [(12-TMC)Co^{III}(OOH)]$^{2+}$ (**2**) (1.0 mM) by addition of acid/base in acetone at –40 °C: UV-vis spectra of **1** (black line), **2** (blue line), after addition of TEA (10 equiv.) to **2** (red line), and after addition of HOTf (10 equiv.) to the species with red line (green line).

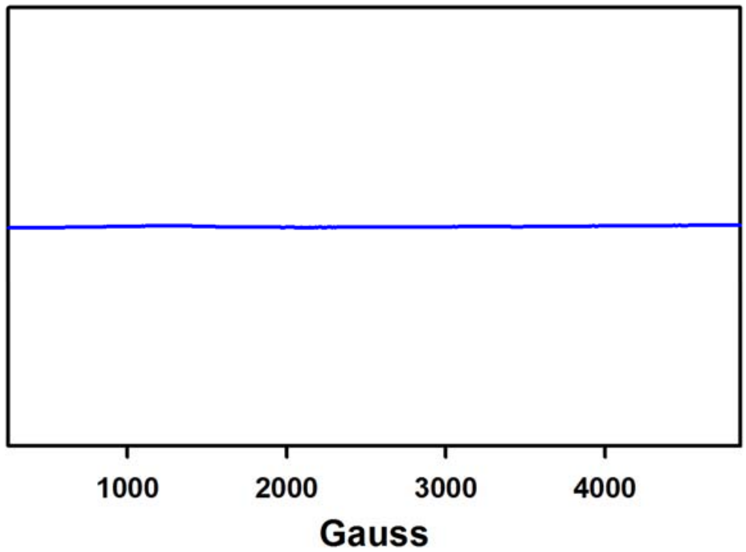

Fig. S3 X-band EPR spectrum of $[(12\text{-TMC})\text{Co}^{\text{III}}(\text{OOH})]^{2+}$ (**2**) (1.0 mM) in acetone at 5 K.

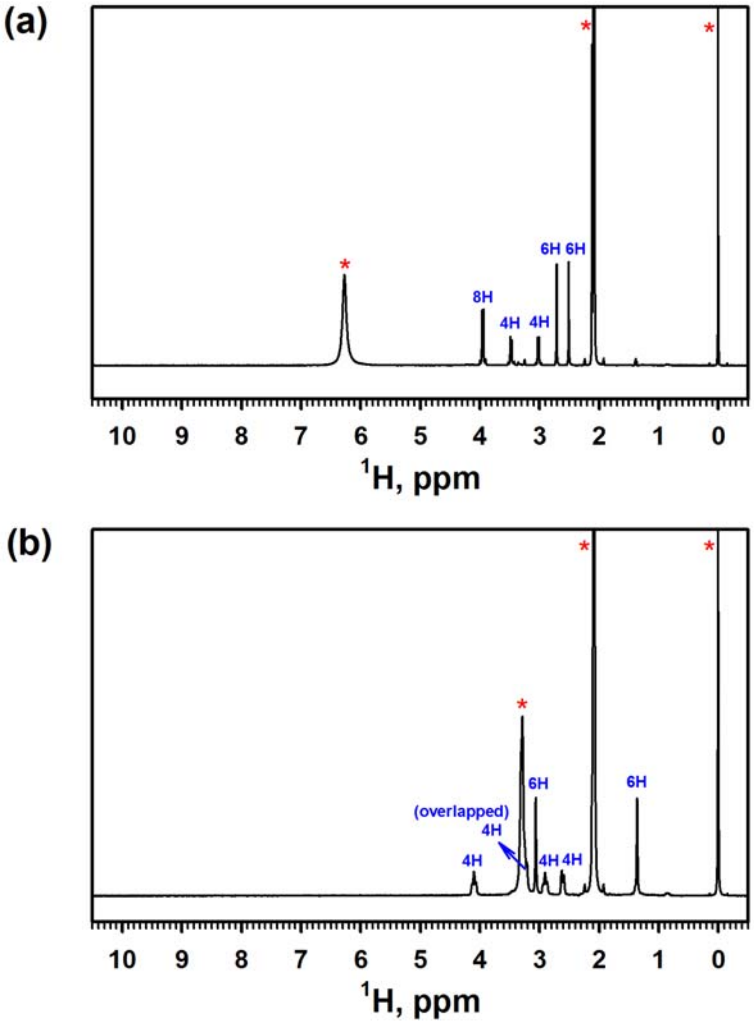

Fig. S4 ^{1}H NMR spectra of (a) $[(12\text{-TMC})\text{Co}^{\text{III}}(\text{OOH})]^{2+}$ (**2**) (1.0 mM) and (b) $[(12\text{-TMC})\text{Co}^{\text{III}}(\text{O}_2)]^{+}$ (**1**) (1.0 mM) in acetone-*d*6 at –30 ºC. The peaks marked with * are from TMS, solvent itself, and water in acetone-*d*6.

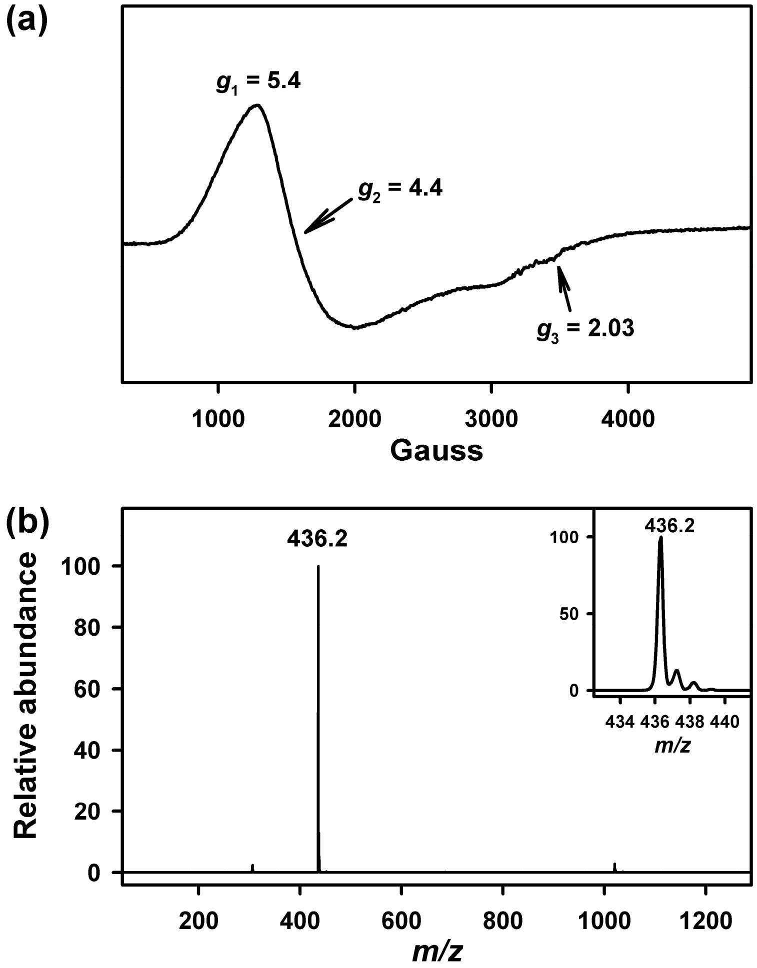

Fig. S5 (a) X-band EPR spectrum of the complete reaction solution obtained in the oxidation of CHD (100 mM) by **2** (1.0 mM) in acetone at 0 °C. Spectrum was recorded at 5 K. (b) ESI-MS spectrum of the complete reaction solution obtained in the oxidation of CHD (100 mM) by **2** (1.0 mM) in acetone at 0 °C. The peak at *m/z* = 436.2 corresponds to $[\mathrm{Co^{II}(12\text{-}TMC)(CF_3SO_3)}]^+$ (*calc. m/z* = 436.1). Inset shows the isotope distribution pattern of the peak at *m/z* = 436.2.

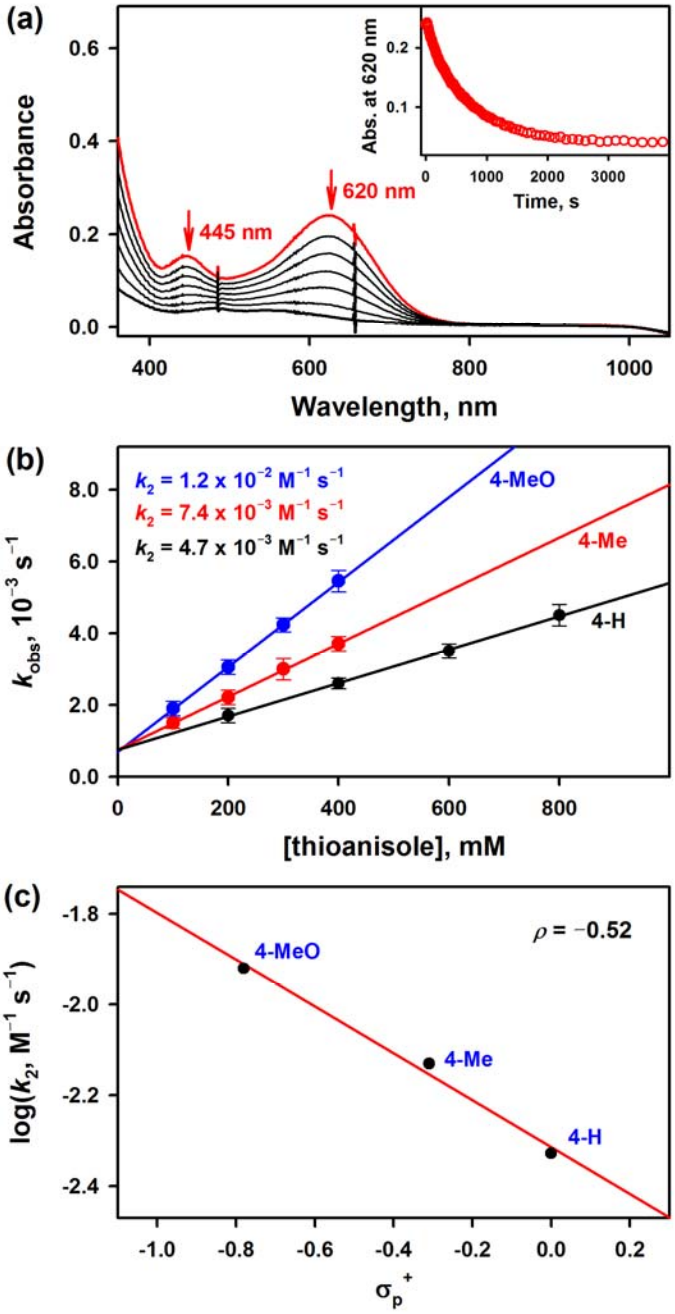

Fig. S6 (a) UV−vis spectral changes observed in the reaction of **2** (1.0 mM) with thioanisole (200 mM) in acetone at 0 ºC. The inset shows the time course monitored at 620 nm. (b) Plots of the pseudo-first-order rate constants (k_{obs}) against concentrations of 4-MeO-thioanisole (blue circles), 4-Me-thioanisole (red circles), and thioanisole (black circles) derivatives, to determine second-order rate constants (k_2) for the oxidation of thioanisole derivatives by **2** in acetone at 0 ºC. (c) Hammett plot of log k_2 against σ_p^+ of 4–X–thioanisoles (X = MeO, Me, and H).

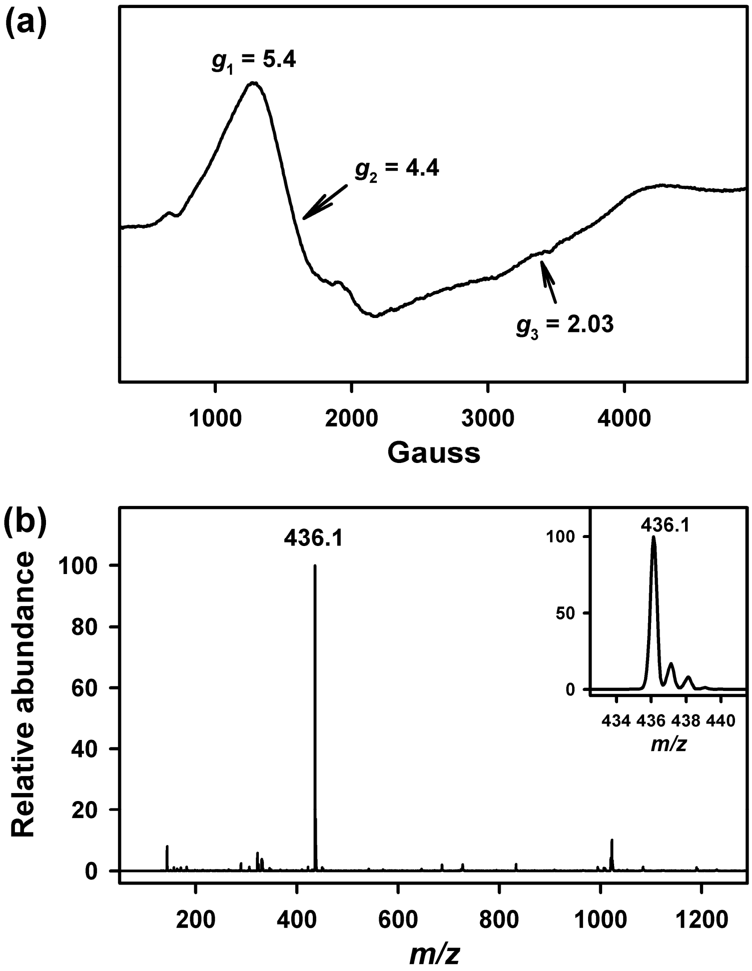

Fig. S7 (a) X-band EPR spectrum of the complete reaction solution obtained in the oxidation of thioanisole (50 mM) by **2** (1.0 mM) in acetone at 0 °C. Spectrum was recorded at 5 K. (b) ESI-MS spectrum of the complete reaction solution obtained in the oxidation of thioanisole (50 mM) by **2** (1.0 mM) in acetone at 0 °C. The peak at *m/z* = 436.1 corresponds to $[\mathrm{Co^{II}}(12\text{-TMC})(\mathrm{CF_3SO_3})]^+$ (*calc. m/z* = 436.1). Inset shows the isotope distribution pattern of the peak at *m/z* = 436.1.

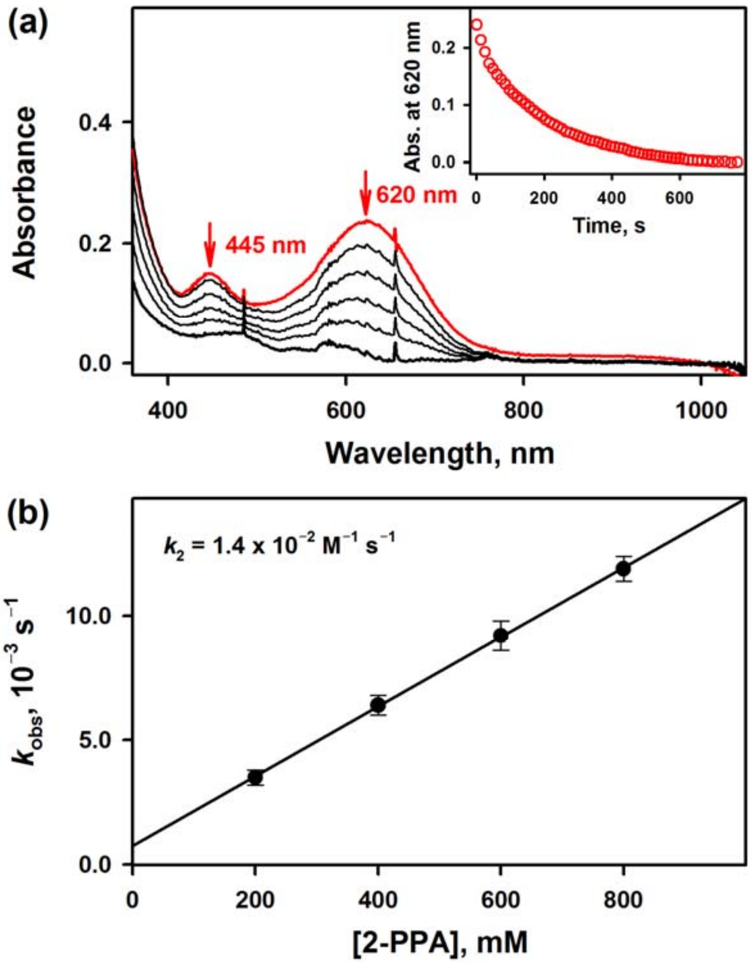

Fig. S8 (a) UV−vis spectral changes observed in the reaction of **2** (1.0 mM) with 2-PPA (400 mM) in acetone at 0 °C. The inset shows the time course monitored at 620 nm. (b) Plot of the pseudo-first-order rate constants (k_{obs}) against 2-PPA concentrations to determine second-order rate constants (k_2) for the oxidation of 2-PPA by **2** in acetone at 0 °C.

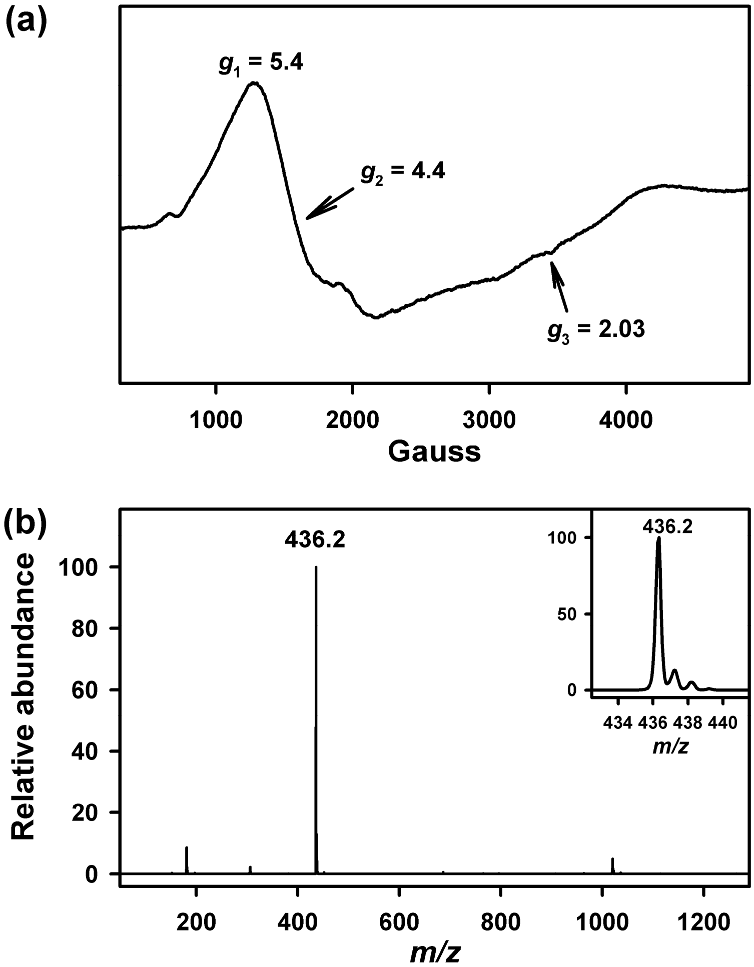

Fig. S9 (a) X-band EPR spectrum of the complete reaction solution obtained in the oxidation of 2-PPA (50 mM) by **2** (1.0 mM) in acetone at 0 °C. Spectrum was recorded at 5 K. (b) ESI-MS spectrum of the complete reaction solution obtained in the oxidation of 2-PPA (50 mM) by **2** (1.0 mM) in acetone at 0 °C. The peak at *m/z* = 436.2 corresponds to $[Co^{II}(12\text{-}TMC)(CF_3SO_3)]^+$ (*calc. m/z* = 436.1). Inset shows the isotope distribution pattern of the peak at *m/z* = 436.2.

Coordinates

The DFT calculated coordinates are given in xyz-file format, with charge/multiplicity given in parenthesis in the comment line.

```
48
(2/1)
Co 0.01124 -0.13308 -0.00494
C -2.39233 0.88399 1.53553
H -3.32898 0.65410 2.06763
H -2.62088 1.46275 0.63292
H -1.76505 1.48026 2.21068
N 1.72383 -0.41041 -1.13590
N -1.69479 -0.37425 1.15874
N 0.93811 -1.29219 1.38199
C 2.65404 -1.29620 -0.34380
H 3.36317 -0.64537 0.18079
H 3.24955 -1.92122 -1.02570
C 1.69084 -0.39617 2.31528
H 1.00273 0.19447 2.92748
H 2.33419 0.29709 1.76493
H 2.31446 -1.01100 2.98304
C -0.10209 -2.03647 2.14122
H 0.30324 -2.41470 3.09390
H -0.40508 -2.91473 1.55900
C -1.26315 -1.09441 2.40768
H -2.11547 -1.63878 2.84187
H -0.97251 -0.33277 3.14131
C 1.89799 -2.15872 0.65208
H 1.33957 -2.96394 0.16218
H 2.60315 -2.63909 1.35041
C 2.43721 0.84244 -1.50404
H 1.75385 1.50028 -2.05183
H 2.77613 1.35770 -0.59844
N -0.92970 -1.23131 -1.37287
C 1.27201 -1.09212 -2.39440
H 0.98966 -0.31072 -3.10987
H 2.10768 -1.64880 -2.84476
C -1.65206 -0.32867 -2.32296
H -2.36692 0.30352 -1.79066
H -0.94619 0.32550 -2.84156
H -2.18814 -0.94654 -3.05898
C -1.90944 -2.08455 -0.65009
H -2.61829 -2.54202 -1.35909
H -1.36772 -2.90489 -0.16729
C -2.64742 -1.21656 0.34987
H -3.26608 -1.83291 1.01886
H -3.33192 -0.53650 -0.17029
C 0.09609 -2.00816 -2.12460
H 0.37805 -2.88714 -1.53414
H -0.32740 -2.38225 -3.07011
H 3.30885 0.60431 -2.13408
O -0.41821 1.52064 -0.73242
O 0.42328 1.81544 0.38551
H -0.15629 2.26639 1.03308
```

```
48
(2/3)
Co 0.06892 -0.06796 0.09656
C -2.35663 0.83499 1.78032
H -3.21086 0.55889 2.42101
H -2.73078 1.43119 0.94101
H -1.65117 1.43920 2.36265
N 1.82817 -0.46841 -1.12720
N -1.68396 -0.38874 1.27882
N 1.02374 -1.33576 1.45038
C 2.72815 -1.35265 -0.32055
H 3.44046 -0.70527 0.20576
H 3.32415 -1.99938 -0.98419
C 1.77751 -0.52144 2.45048
H 1.09547 0.13190 3.00582
H 2.52009 0.11035 1.95126
H 2.29048 -1.19210 3.15798
C -0.05585 -2.11057 2.12590
H 0.32411 -2.57686 3.04995
H -0.35940 -2.93084 1.46462
C -1.22224 -1.19498 2.45781
H -2.06201 -1.78317 2.86176
H -0.93005 -0.48377 3.24068
C 1.95815 -2.19877 0.67862
H 1.37328 -2.97959 0.17878
H 2.65946 -2.71298 1.35695
C 2.55685 0.76255 -1.50984
H 1.88316 1.43850 -2.04955
H 2.92325 1.27564 -0.61189
N -0.97105 -1.17670 -1.44332
C 1.31396 -1.13827 -2.36259
H 1.08630 -0.34755 -3.08890
H 2.10656 -1.75987 -2.81007
C -1.66201 -0.28966 -2.41094
H -2.37190 0.36925 -1.89904
H -0.93772 0.34615 -2.93050
H -2.20845 -0.89819 -3.15079
C -1.94898 -1.98797 -0.67969
H -2.72298 -2.40592 -1.34654
H -1.42528 -2.84757 -0.24406
C -2.63337 -1.14441 0.39242
H -3.28469 -1.78557 1.00757
H -3.28232 -0.40202 -0.08777
C 0.06891 -1.98316 -2.12367
H 0.28953 -2.86430 -1.50830
H -0.29741 -2.36682 -3.09143
H 3.41425 0.51338 -2.15795
O -0.03371 1.57577 -0.71196
O -0.52873 2.57975 0.09261
H -1.30057 2.91598 -0.40581
```

```
48
(2/5)
Co 0.07399 -0.01937 0.08097
C -2.41051 0.75382 1.82199
H -3.27838 0.49003 2.45098
H -2.75950 1.37672 0.98855
H -1.70365 1.33854 2.42560
N 1.84133 -0.45910 -1.17670
N -1.74054 -0.46420 1.30136
N 1.04191 -1.32812 1.49996
C 2.73514 -1.30252 -0.32617
H 3.42391 -0.62263 0.19202
H 3.35764 -1.95994 -0.95655
C 1.75870 -0.53422 2.53328
H 1.05184 0.09670 3.08506
H 2.50134 0.12401 2.06527
H 2.27166 -1.20514 3.24296
C -0.03697 -2.13944 2.11996
H 0.32193 -2.62765 3.04279
H -0.30178 -2.94720 1.42704
C -1.25257 -1.27987 2.45090
H -2.06069 -1.92256 2.84020
H -0.99561 -0.58126 3.25817
C 1.99100 -2.14905 0.70415
H 1.42448 -2.95262 0.21752
H 2.72812 -2.64322 1.36085
C 2.58283 0.75114 -1.61350
H 1.93087 1.39078 -2.22167
H 2.91421 1.32173 -0.73571
N -0.99744 -1.17296 -1.42302
C 1.30625 -1.17432 -2.37311
H 1.08125 -0.41324 -3.13181
H 2.07970 -1.83056 -2.80730
C -1.69152 -0.31526 -2.41464
H -2.44865 0.30461 -1.92121
H -0.97988 0.35448 -2.91051
H -2.18416 -0.94124 -3.17766
C -1.97452 -2.00825 -0.67809
H -2.73056 -2.42941 -1.36336
H -1.43907 -2.86404 -0.24955
C -2.67847 -1.19972 0.40541
H -3.33444 -1.86501 0.99236
H -3.33209 -0.45415 -0.06603
C 0.05144 -1.99316 -2.08795
H 0.27604 -2.85193 -1.44341
H -0.32815 -2.41193 -3.03618
H 3.46779 0.47505 -2.21270
O -0.42602 1.75875 -0.73567
O -0.36391 2.82366 0.04643
H -0.58148 3.58549 -0.53809
```